Published in final edited form as:
J Comp Neurol. 2011 December 15; 519(18): 3640–3656. doi:10.1002/cne.22756.

Immunohistochemical Identification and Synaptic Inputs to the Diffuse Bipolar Cell Type DB1 in Macaque Retina

Theresa Puthussery[1,*], **Jacqueline Gayet-Primo**[1], **W. Rowland Taylor**[1], and **Silke Haverkamp**[2]

[1]Casey Eye Institute, Department of Ophthalmology, Oregon Health and Sciences University, Portland, Oregon 97239

[2]Max Planck Institute for Brain Research, D-60528 Frankfurt a.M., Germany

Abstract

Detailed analysis of the synaptic inputs to the primate DB1 bipolar cell has been precluded by the absence of a suitable immunohistochemical marker. Here we demonstrate that antibodies for the EF-hand calcium-binding protein, secretagogin, strongly label the DB1 bipolar cell as well as a mixed population of GABAergic amacrine cells in the macaque retina. Using secretagogin as a marker, we show that the DB1 bipolar makes synaptic contact with both L/M as well as S-cone photoreceptors and only minimal contact with rod photoreceptors. Electron microscopy showed that the DB1 bipolar makes flat contacts at both triad-associated and nontriad-associated positions on the cone pedicle. Double labeling with various glutamate receptor subunit antibodies failed to conclusively determine the subunit composition of the glutamate receptors on DB1 bipolar cells. In the IPL, DB1 bipolar cell axon terminals expressed the glycine receptor, GlyRα1, at sites of contact with AII amacrine cells, suggesting that these cells receive input from the rod pathway.

Keywords

secretagogin; OFF cone bipolar cells; cone photoreceptors; blue cone input; glutamate receptors; amacrine cell; glycine receptor

One of the major hurdles to advancing our understanding of nervous system function is obtaining a complete description of the various neural pathways, including elaborating the specific synaptic connections between identified neurons, and establishing the transmitter systems that mediate those connections. The retina has proved particularly amenable to such efforts, due in large part to the discovery of numerous cell-type-specific immunohistochemical markers, in combination with antibodies against neurotransmitter receptors. A great deal of comparative data shows that neural pathways are often well conserved across mammalian and other vertebrate species.

At the first synapse in the retina, glutamate released from cone photoreceptors activates receptors in the dendrites of bipolar cells, the feedforward excitatory neurons, and the horizontal cells, which provide lateral inhibitory connections. Two types of bipolar cell, ON and OFF, encode increments and decrements in light intensity, respectively. All OFF bipolar cells are depolarized by glutamate because they express ionotropic glutamate receptors that

[*]CORRESPONDENCE TO: Casey Eye Institute, Department of Ophthalmology, Oregon Health and Sciences University, 3375 SW Terwilliger Blvd., Portland, OR, 97239. puthusse@ohsu.edu.

Additional Supporting Information may be found in the online version of this article.

are preferentially gated by either α-amino-3-hydroxy-S-methylisoxazole-4-propionic acid (AMPA, GluA1-4, formerly GluR1-4), or kainate (KA, GluK1-5, formerly GluR5-7, KA1-2). Previous studies in the ground squirrel retina suggest that the temporal response properties of OFF bipolar cells may be influenced by the type of glutamate receptor expressed in their dendrites (DeVries, 2000). In the macaque retina, the OFF bipolar cells comprise four distinct types that can be identified based on the stratification pattern of their axon terminals in the outer part of the inner plexiform layer (IPL; Boycott and Wässle, 1991). Of these, three types of diffuse bipolar (DB) cells, DB1, DB2, and DB3, make multiple connections to cone photoreceptors, while a fourth type, the flat midget bipolar (FMB) cell, makes one-to-one connections with cone photoreceptors in the central retina.

Early Golgi studies combined with electron microscopy provided initial clues about the connectivity of individual bipolar cell types in the primate retina (Dowling and Boycott, 1966; Kolb, 1970; Boycott and Hopkins, 1993). However, the discovery of immunohistochemical markers to stain specific bipolar cell types significantly accelerated progress. In the macaque retina, DB2 cells are labeled with antibodies against GLT-1, DB3 cells are labeled with calbindin antibodies, and FMB cells are labeled with recoverin antibodies (Grünert et al., 1994; Wässle et al., 1994; Jacoby et al., 2000). Until now, a marker of the DB1 cell has remained elusive. Previously, we demonstrated that the calcium-binding protein, secretagogin (SCGN), labels numerous subtypes of cone bipolar cell in the mouse, rat, and rabbit retina (Puthussery et al., 2010). Secretagogin is a recently identified member of the EF-hand family of calcium-binding proteins that is expressed in various brain regions and peripheral tissues (Wagner et al., 2000). Here we demonstrate that secretagogin is a marker of the DB1 bipolar cell in the macaque retina. We have utilized this marker to investigate the cone connectivity, glutamate receptor expression, and synaptic inputs to the DB1 bipolar cell.

MATERIALS AND METHODS

Animals and tissue preparation

Four retinas were collected from three adult cynomolgus macaque monkeys (*Macaca fascicularis*) that were euthanized after electrophysiological experiments unrelated to those described here. All procedures were approved by the local Animal Care Committee and were in accordance with the law for animal experiments issued by the German government (Tierschutzgesetz). In addition, three retinas from three adult rhesus macaques (*Macaca mulatta*) were collected postmortem as part of the Tissue Distribution Program at the Oregon National Primate Research Center. No differences in staining were observed between the two species. The anterior segment and vitreous were removed from the eye and the posterior eyecup was immersion-fixed in 4% paraformaldehyde in 0.1 M phosphate buffer (PB, pH 7.4) for 5–60 minutes at 25 °C. Although the secretagogin antibody worked well across this range of fixation times, lighter fixation was necessary to obtain good staining with the glutamate and glycine receptor antibodies. Following fixation, retinas were dissected from the eyecups, cryoprotected in graded sucrose solutions (10%, 20%, 30%), and stored at –20 °C for later use. For light microscopy, samples of retina were used as a wholemount or sectioned vertically (12–16 μm) or horizontally (20–30 μm) with a cryostat. Retinal eccentricities were defined as follows: up to 2 mm from fovea (first 10° of visual angle) was denoted “central,” from 2–6 mm was denoted “mid-peripheral,” and >6 mm from the fovea was denoted “peripheral.”

The tissue used for electron microscopy was immersion-fixed in 4% paraformaldehyde for 60 minutes. After cryoprotection the tissue was frozen and thawed and vertical vibratome sections (60 μm) were cut for preembedding immunoelectron microscopy.

Antibody characterization

A list of the primary antibodies used in this study is shown in Table 1. The noncommercial secretagogin antibody (gift from Ludwig Wagner) recognizes a single band of the predicted size (≈32 kDa) on western blots of mouse retinal lysates (Puthussery et al., 2010). The pattern of staining obtained with both of the commercial antibodies was identical to that obtained with the noncommercial antibody.

We used an antibody against β-dystroglycan to label the terminals of rods and cones in primate retina. It recognizes a band of 43 kDa in western blots of human retina (Drenckhahn et al., 1996).

The mouse anti-calbindin D-28K antibody recognizes a 28 kDa band in western blots of mouse renal proteins. The pattern obtained here was similar to previous studies in macaque retina (Grünert et al., 1994).

The goat anti-calretinin antibody detects an ≈30 kDa band on western blots of rat brain extracts (Winsky et al., 1996). The pattern of staining was consistent with previous reports (Wässle et al., 1995; Kolb et al., 2002).

Staining with the guinea pig anti-gamma-aminobutyric acid (GABA) antibody is blocked by preadsorption with 100 μm GABA coupled to glutaraldehyde. Staining is not blocked by preadsorption with 500 μm of glutamate or taurine (manufacturer's data sheet).

Antibodies against the glutamate receptor subunits GluA1, GluA4, and GluK2/3 have been tested in western blots of rat retina: the GluA1 and GluA4 antisera each detect a single band of 100 kDa (Hack et al., 1999) and the GluK2/3 antiserum detects a single band of ≈110 kDa (Brandstätter et al., 1997). The GluA2 antiserum has been tested by western blot of partially purified rat hippocampal brain lysates showing a single band of ≈106 kDa (manufacturer's datasheet and technical information). The specificity of the GluK1 antiserum has been tested in western blot of mouse brain lysates, revealing a single band at the predicted size of ≈104 kDa (Park et al., 2010). The staining pattern of these three antibodies has been well described in primate retina (Haverkamp et al., 2000, 2001a,b; Puller et al., 2007), while the pattern of staining obtained with the GluA2 antibody was consistent with that previously reported in primate retina (Haverkamp et al., 2001a).

The rabbit anti-GLT-1 antibody recognizes a band of ≈65 kDa in western blots of rat brain homogenates. It recognizes rat EAAT and crossreacts with human and mouse homologs. GLT-1 labels OFF bipolar cells in primate retina (Lee and Grünert, 2007).

The mouse anti-glycine receptor antibody clone mAb2b recognizes a band of ≈48 kDa in western blots of purified rat spinal cord GlyR preparations (Pfeiffer et al., 1984) and has been shown to be specific for the N-terminal 10 residues of the GlyRα1 subunit (Schroder et al., 1991). This antibody labels glycinergic synapses in the IPL of the macaque retina (Jusuf et al., 2005).

The specificity of the rabbit anti-GlyT1 antibody has been previously demonstrated by western blots in rat retinal and spinal cord homogenates. It recognizes a single band of 68 kDa (Pow and Hendrickson, 1999).

The mouse anti-$G\alpha_o$ antibody recognizes human, bovine, guinea pig, rat, and mouse $G\alpha_o$ and does not crossreact with transducin, $G\alpha_i$, or $G\alpha_s$ subunits. Specificity and crossreactivity analysis was determined by western blot using purified proteins. The antibody detects a single band of ≈39–42 kDa in bovine and rat membranes (manufacturers

datasheet and correspondence). The pattern of staining here was identical to that obtained previously in macaque retina (Vardi, 1998).

ON bipolar cells were labeled with a polyclonal antibody directed against anti-Gγ13 that was raised in rabbit against a peptide (amino acid 47–59) of mouse Gγ13 and whose specificity was established by correlating in situ hybridization and immunostaining in murine lingual tissue (Huang et al., 1999, 2003). The staining pattern in macaque is consistent with the staining pattern in mouse retina (Dhingra et al., 2008).

The rat-anti-Rec1 antibody detects a 23 kDa band on western blots of purified bovine recoverin (Adamus and Amundson, 1996). The staining pattern was consistent with previous studies in macaque retina (Milam et al., 1993; Wässle et al., 1994).

The rabbit anti-S-opsin antibody JH455 has been characterized by Wang et al. (1992) by staining of transfected tissue culture cells and western blots. The antibody stained cells expressing recombinant human S-cone pigment and not those expressing recombinant human M/L cone pigment. For the western blots, the S-cone opsin antibody bound specifically to recombinant human blue pigment, but not to recombinant human red/green pigments. JH455 labels the whole S-cone population including their cone pedicles in primate retina (Martin and Grünert, 1999).

The mouse monoclonal anti-tyrosine hydroxylase antibody recognizes a 59–61 kDa band by western blot of mouse brain lysates (manufacturers data sheet). Staining obtained here was similar to previous reports in macaque retina (Hokoc and Mariani, 1987; Mariani and Hokoc, 1988).

The guinea pig anti-vGluT1 detects a 62 kDa band on western blots of rat brain lysates (manufacturers data sheet). vGluT1 labels synaptic terminals of photoreceptors and bipolar cells and the localization pattern is highly conserved across mammalian species (Johnson et al., 2003; Gong et al., 2006). The pattern of staining obtained here was consistent with previous reports.

Indirect immunofluorescence immunohistochemistry

For immunohistochemistry on vertical sections, nonspecific binding sites were blocked with an incubation buffer (IB) containing 3% normal horse serum (NHS), 0.3% Triton X-100, and 0.025% NaN_3 in 0.1 M phosphate-buffered saline (PBS; pH 7.4) for 10 minutes. Primary antibodies were diluted in IB and applied to tissues for 2 hours (or overnight) at 25°C. Secondary antibodies were conjugated to Alexa Fluor 488, 594, 647 (Molecular Probes, Eugene, OR) or Cy3 (Dianova, Hamburg, Germany) and were raised in donkey, with the exception of the anti-guinea pig secondary antibodies, which were raised in goat. Secondary antibodies were applied to sections for 1 hour at 25°C (1:500–1:800 in IB). For double or triple labeling experiments, sections were incubated in a mixture of primary antibodies followed by a mixture of secondary antibodies. For retinal wholemount staining, the concentration of Triton X-100 in the IB was increased to 1% and antibodies were applied for 7–10 days at 25°C. Wholemounts were washed for 3–5 hours and secondary antibodies were applied overnight at 25°C.

Confocal images were taken using a Zeiss LSM 5 Pascal or an Olympus Fluoview 1000 confocal microscope equipped with an argon and an HeNe laser. Scanning of confocal image stacks was performed with a Plan-Apochromat 63 ×/1.40 oil (Zeiss), an Olympus Plan Apo 60 ×/1.42 oil or an Olympus UPlan FLN 40×/1.3 oil objective at 1024 × 1024 or 1024 × 768 pixels. When projections of image stacks are shown, serial optical sections were collapsed into a single image plane. The number of images and the z spacing interval is

noted in the legend for each figure. Brightness and contrast of the final images were adjusted using Adobe Photoshop CS or CS3 (San Jose, CA).

Preembedding immunoelectron microscopy

Vibratome sections were blocked for 1 hour in PBS containing 10% NHS and 1% bovine serum albumin (BSA). Tissue sections were incubated in Biovendor rabbit antisecretagogin diluted 1:5,000 with 3% NHS, 1% BSA, and 0.02% NaN_3 in PBS for 4 days at 4°C. Biotinylated goat anti-rabbit IgG was applied as secondary antibody (1:100; Vector, Burlingame, CA), and a peroxidase-based enzymatic detection system (Vectastain Elite ABC kit; Vector) was used to visualize antibody binding. The sections were then postfixed with 2.5% (v/v) glutaraldehyde in cacodylate buffer for 1 hour. The product of the enzyme reaction was silver intensified. The sections were then incubated in 0.5% (w/v) osmium tetroxide for 30 minutes at 4 °C. Dehydration was carried out by an ethanol series and propylene oxide. Specimens were embedded in Epon and a series of ultrathin sections (60 nm) were collected on copper grids and stained with uranyl acetate and lead citrate. Ultrathin sections were examined with a Zeiss EM10 electron microscope and photographed with a Bio-Scan digital camera (Gatan, Munich, Germany) in combination with the software program Digital Micrograph 3.1 (Gatan, Pleasanton, CA). Images were adjusted as described above.

Nearest-neighbor analysis and axonal arbor measurements

Nearest-neighbor analysis was performed as described previously (Wässle and Riemann, 1978). Confocal image stacks were collected with the focal plane extending from the outer plexiform layer (OPL) to the inner nuclear layer (INL). We analyzed five fields, each measuring 240 × 180 μm^2, from mid-peripheral retina. Bipolar cells were distinguished from amacrine cells by tracing each cell soma to its dendrites in the OPL. All of the analyzed cells had a similar staining intensity. The distance between the center of each SCGN-positive bipolar soma and its nearest neighbor was measured with ImageJ software and statistics were performed with Graphpad Prism v. 4.0 for Mac (Graphpad Software, La Jolla, CA). To determine the width of bipolar cell axonal arbors, we acquired confocal z-stacks from peripheral wholemount retinas stained for SCGN and recoverin. Images were collected from the level of the axons to the axon terminal. Only cells for which individual arbors could be discriminated were analyzed. We measured the width of the axonal arbor across the longest axis using ImageJ software.

Localization of GlyRα1 puncta at contacts between DB1 and AII amacrine cells

We used calretinin as a marker of AII amacrine cells. It should be noted that although 70% of calretinin-positive amacrine cells in macaque are AII amacrine cells, an additional population of glycinergic amacrine cells also stain with this antibody (Kolb et al., 2002). In vertical sections from the central retina, we observed numerous calretininimmunoreactive cells with small somata, which probably represented the non-AII glycinergic amacrine cell type reported by Kolb et al. (2002). In contrast, in more peripheral retinal regions most of the calretinin-positive amacrine cells had larger somas and morphology consistent with the AII amacrine cell. Thus, we performed our triple labeling studies on sections from more peripheral retinal regions to reduce the chances of encountering calretinin-immunore-active non-AII cells. Confocal stacks were acquired to encompass the DB1 soma, axon, and axon terminals. Once such cells were identified, we evaluated single optical sections within the image stack to identify sites of colocalization between SCGN, GlyRα1, and calretinin.

RESULTS

Localization of SCGN in the primate retina

We evaluated the localization of SCGN in vertical sections and wholemounts from a peripheral region of the macaque retina. The overall pattern of SCGN expression was quite different from that reported previously in the mouse, rat, and rabbit retina, where SCGN labeled most cone bipolar cell types (Puthussery et al., 2010). Vertical sections showed strong immunoreactivity in a subpopulation of cone bipolar cells, with staining present in the soma, dendrites, axon, and axon terminals (Fig. 1A) (see Table 2 for figure abbreviations). In addition, we observed SCGN in a sparse population of amacrine cells and in some cells with somata located in the ganglion cell layer (Fig. 1A, arrows). In the IPL a single confocal section shows SCGN-immunoreactive processes predominantly localized to strata (S) 1 and S5 of the IPL with a weaker band of processes evident in S3 (Fig. 1B). Double labeling for SCGN and vGluT1, a marker of glutamatergic bipolar cell axon terminals, was performed to determine where the SCGN-positive bipolar cells terminated in the IPL (Fig. 1C). Superimposition of SCGN and vGluT1 staining was observed only in S1. Other bands of SCGN-immunoreactive processes were observed in S1, S2, S3, and S5, but these processes lacked vGluT1 immunoreactivity and were therefore unlikely to originate from bipolar cells. We observed the same pattern of staining with all three of the polyclonal SCGN antibodies that we tested. The diffuse arborization of the bipolar cell dendrites in the OPL was very obvious in wholemounts (Fig. 1D). In sublamina a of the IPL, we observed SCGN-immunoreactive terminals that also showed vGluT1-immunoreactivity (Fig. 1F, white, arrows). These terminals were rather fine and were interspersed with swellings arranged like “pearls on a string.” In contrast, the other vGluT1-positive axon terminals seen at the same focal plane were relatively larger and more bulbous, and were most likely axon terminals of flat midget and DB2 bipolar cells (see Golgi-stained bipolar cells in Boycott and Wässle, 1991). Figure 1G,H show examples of SCGN-positive putative amacrine cells with nuclei in the INL and GCL, respectively. These cells were morphologically diverse, suggesting that multiple populations were stained. Some of these cells had dendrites spanning over 500 μm.

SCGN is expressed in dopaminergic amacrine cells and other wide-field GABAergic amacrine cells

We sought to identify the types of amacrine cells stained with SCGN in the INL and to determine whether SCGN-positive cells in the GCL were amacrine or ganglion cells (Fig. 2). Double labeling for the glycine transporter-1 (GlyT1) and SCGN showed no colocalization (Fig. 2A–C), suggesting that none of the SCGN-positive amacrine cells were glycinergic. In contrast, all of the SCGN-stained somata in the proximal INL and in the GCL were also immunoreactive for GABA (Fig. 2D–F). These data indicate that SCGN is expressed by both conventionally placed and displaced amacrine cells. It is unlikely that SCGN is expressed in ganglion cells, since these neurons typically show low levels of GABA immunoreactivity (Kalloniatis et al., 1996). We then double-labeled for SCGN and tyrosine hydroxylase, a marker of dopaminergic amacrine cells (Hokoc and Mariani, 1987), since these amacrine cells are also known to show GABA immunoreactivity (Wässle and Chun, 1985). Figure 2G–J shows that both conventionally placed and displaced dopaminergic amacrine cells are also SCGN-immunoreactive. However, numerous other SCGN-positive amacrine cells were observed that were not immunoreactive for TH. Thus, SCGN is likely to be expressed by multiple types of GABAergic amacrine cell in the macaque retina.

SCGN is expressed by DB1 bipolar cells

To gain an insight into the type of bipolar cells that were labeled with SCGN, we first double-labeled for the G-protein subunit, $G\alpha_o$, which is expressed in ON-type, but not OFF-type, bipolar cells (Vardi, 1998). All of the intensely labeled SCGN-positive bipolar cells lacked immunoreactivity for $G\alpha_o$, indicating that they were OFF bipolar cells (Fig. 3A–C, but see Fig. 7F,G).

To determine which OFF bipolar cell types expressed SCGN, we double-labeled with established markers of monkey OFF bipolar cells. Figure 3D–F shows a vertical section stained for SCGN and the calcium-binding protein recoverin, which selectively stains FMB cells in the macaque retina (Milam et al., 1993; Wässle et al., 1994). The SCGN-positive bipolar cells did not show recoverin immunoreactivity, and their terminals were typically located distal to the FMB cells. Next, we double-labeled for SCGN and the glutamate transporter GLT-1 (EAAT2), which has previously been shown to label DB2, FMB, and possibly DB1 cells in the macaque (Grünert et al., 1994) (Fig. 3G–I). The SCGN-positive cells showed weak GLT-1 immunoreactivity; however, the DB2 axon terminals, which were strongly labeled for GLT-1, showed no SCGN immunoreactivity. The SCGN-positive axon terminals were located more distally to the DB2 axon terminals. Finally, we double-labeled for SCGN and calbindin (Fig. 3J–L), another EF-hand calcium-binding protein that is a marker for DB3 cells (Grünert et al., 1994). The DB3 cells stratify narrowly in the proximal aspect of S2 of the IPL. The axon terminals and somata of the DB3 cells were not immunoreactive for SCGN. Overall, the morphology and stratification, taken together with the lack of colocalization with other known OFF bipolar cell markers, indicates that the SCGN-positive bipolar cells are likely the DB1 cell originally described in the classification scheme of Boycott and Wässle (1991).

We performed a nearest-neighbor analysis to determine whether the SCGN-positive bipolar cells represent a homogeneous population that tile the retina in a regular mosaic (Fig. 4) (Wässle and Riemann, 1978). Analysis of the soma positions showed a mean distance to nearest neighbor of 14.16 ± 4.027 μm (SD). The regularity index (mean/SD) was 3.52 (Fig. 4B). The nearest-neighbor distances were well fitted by a Gaussian distribution, indicating that these cells form a nonrandom, regular mosaic.

We also quantified the relative soma position of the DB1 cells in vertical sections taken from various locations in mid-peripheral and peripheral retina. The distance from the cone pedicles to the center of each DB1 soma was measured and expressed as a percentage of total INL thickness (0%, OPL; 100%, IPL). The DB1 somata were positioned at a relative depth of 54% ± 8% (mean ± SD, $n = 88$ cells), and are thus positioned in approximately the middle of the INL.

The axon terminals of individual DB1 cells were difficult to delineate from neighboring cells, which precluded the assessment of axonal arbor size in a large sample of cells. However, in wholemounts of peripheral retina stained for SCGN and recoverin, we could determine the spatial extent of individual axon arbors for a small number of cells. The width of the DB1 axonal arbor along the longest axis was ≈46.7± 2.3 μm ($n = 6$) compared with 15 ± 0.6 μm ($n = 8$) for the FMB axon terminal (data not shown). These values are in accord with previous estimates for these cell types (see fig. 4, Boycott and Wässle, 1991).

Rod and cone connectivity of DB1 bipolar cells

Most of the diffuse bipolar cells in the primate retina are biased against S-cone contacts (Lee and Grünert, 2007), and, interestingly, the putative homologs of the DB1 bipolar in mouse (type-1, Ghosh et al., 2004) and ground squirrel (cb1 or former b7, Puller et al., 2011) are most likely M-cone selective (Breuninger et al., 2011; Li and DeVries, 2006). To determine

the amount of S-cone input for DB1 cells, we double-labeled vertical sections and wholemounts with antibodies against SCGN and S-opsin (Fig. 5A,B). We found several examples of S-cone pedicles innervated by SCGN-labeled dendrites and saw no obvious bias of DB1 dendritic endings toward M/L-versus S-cone pedicles.

Next, we evaluated whether DB1 bipolar cells receive direct rod input. Up to now, there is no evidence for direct contacts between rod terminals and cone bipolar cell dendrites in the primate retina. However, in several other species, rods are directly connected with a subset of cone bipolar cells and provide an alternative pathway for rod signal flow (Hack et al., 1999; Tsukamoto et al., 2001; Fyk-Kolodziej et al., 2003; Li et al., 2004, 2010; Mataruga et al., 2007; Haverkamp et al., 2008). We used β-dystroglycan to label both rod and cone terminals (Drenckhahn et al., 1996). Examples of DB1 bipolar dendrites that made contact with rod spherules are shown in Figure 5C,D. These rod-contacting dendrites were continuous with dendritic branches that also made contacts with cones (Fig. 5C enlargement). Such rod contacts were infrequently observed; in the vertical section shown in Figure 5C we could trace the dendritic trees of eight DB1 cells and only a single rod contact from one DB1 cell was observed. Similarly, in wholemount view we could trace 19 DB1 cells and only one of these cells made a single rod contact. Conversely, in a field containing 2,571 rods, only a single rod was connected with a DB1 bipolar. Thus, it seems likely that rod contacts are an aberration rather than a typical input to the DB1 circuit.

Finally, we analyzed the number of cone contacts and the bipolar cell density in wholemounts from mid-peripheral retina, and calculated the convergence of cones onto individual DB1 bipolar cells, and the divergence of cones onto DB1 bipolar cells, i.e., the number of DB1 bipolar cells that contact each cone. Cone pedicles were labeled with antibodies against GluK1 (Fig. 6B). The DB1 cells analyzed in this area were in contact with 6–8 cones. The histogram in Figure 6C shows the frequency of cone contacts, which ranged from 4 to 9 with a mean convergence of 6.4 ± 1.15 (±SD, $n = 85$). Figure 6D presents an analysis of the cone contacts of six DB1 cells: the dendritic trees of the cells show considerable overlap, several cone pedicles are contacted by two to three DB1 cells, while one cone is contacted by four DB1s. The density of DB1 cells was 1,636 ± 336/mm^2 (mean ±SD, $n = 10$ fields, each of 240 ×240 μm), and the cone density was 5,148 ± 690/mm^2, and therefore there are 3.1 ± 0.4 times more cones than DB1 cells. Each DB1 cell contacted a mean of 6.4 cones, indicating a coverage factor of 6.4/3.1 = 2.1. Our results are in line with a previous estimate of 1,382 DB1 cells per mm^2, five to eight cone pedicles contacted by each DB1 ($n = 8$) and a coverage of 1.6 (Boycott and Wässle, 1991).

Ultrastructural evaluation of DB1 synapses in the OPL

OFF bipolar cells are known to make flat contacts at the base of the cone pedicles, while the horizontal cell and ON bipolar cell processes make invaginating contacts close to the synaptic ribbon in an arrangement known as the triad (Dowling and Boycott, 1966). OFF bipolar cell dendrites are considered to be triad-associated (TA) or nontriad-associated (NTA) depending on whether or not they are positioned adjacent to the triad. Using preembedding immunoelectron microscopy, we were able to determine the position of the DB1 dendrites relative to the synaptic triad. Altogether, a total of 50 contacts were counted; of these, 31 were NTA (Fig. 7A,B) and 19 were TA (Fig. 7C). No rod contacts were observed at the ultrastructural level. Hopkins and Boycott (1996) found that the dendrites of a Golgistained DB1 cell were postsynaptic to seven cones at 71 basal contacts; in addition, the DB1 made two invaginating contacts with one cone and one with another. We also occasionally (≈5 contacts observed at single sections through 40 different cone pedicles) observed clear examples of invaginating processes (Fig. 7D), but it seemed likely that these were ON bipolar cells since the immunolabeling was generally weaker in comparison to the strongly labeled processes making flat contacts (Fig. 7A–C). To test this possibility, we

double-labeled sections for Gγ13, a marker for ON bipolar cells (Huang et al., 2003). We observed that some bipolar cells that were immunoreactive for Gγ13 were also weakly SCGN-positive (Fig. 7E–G, arrow). Such cells constituted ≈5% (8/155) of all cells. These cells showed weak immunoreactivity in the soma and dendrites compared with the DB1 cells and showed no SCGN immunoreactivity in their axon terminals (consistent with a lack of SCGN and vGluT1 superimposition in the ON sublamina in Fig. 1C).

Glutamate receptors of DB1 bipolar cells

In macaque retina, OFF bipolar cells express at least three different types of glutamate receptors: AMPA receptors containing the GluA1 subunit (Haverkamp et al., 2000), kainate receptors containing the GluK1 subunit, and kainate receptors containing the GluK2/3 subunit (Haverkamp et al., 2001b); however, it is not known which bipolar cell types express which receptor subunits. Only the AMPA receptor subunit GluA1 has been definitively localized to the FMB cells, in the marmoset retina (Puller et al., 2007). In view of the strong dendritic labeling of DB1 cells, we attempted to identify the types of glutamate receptors on these cells. We double-labeled vertical and horizontal sections through macaque retina for GluA1 (Fig. 8A–E), GluK1 (Fig. 8F–J), and GluK2/3 (Fig. 8K–O). Some GluR clusters (independent of subunit) were close to SCGN-labeled dendrites; however, overlap was rarely observed, and no individual subunit was reliably detected at the majority of DB1 dendritic endings. Similarly, the dendritic tips of the DB1 bipolars did not show clear colocalization with the GluA2 or GluA4 subunits in vertical retinal sections (see Supplementary Fig. 1). Thus, from these results the subunit composition of the DB1 bipolar remains unknown; however, it seems unlikely that a single glutamate receptor subunit is expressed at the majority of dendritic tips. This is in contrast to the expression of GluA1 by the FMB cells, where over half of the FMB dendritic tips at each cone pedicle were clearly colocalized with GluA1 puncta (Puller et al., 2007).

DB1 bipolar cells express a1 glycine receptor subunits at contacts with AII amacrine cells

The circuitry of the mammalian rod pathway is well established; rods contact rod bipolar cells, which output onto the AII amacrine cell. The signal is subsequently relayed from AII amacrine cells to ON cone bipolar cells via gap junctions, and to OFF bipolar cells via a conventional glycinergic synapse (for review, see Bloomfield and Dacheux, 2001); however, it is not known whether all or only a subset of OFF bipolar cells receive this glycinergic input. To determine whether DB1 bipolar cells receive AII amacrine cell input, we triple-labeled with SCGN, the α1 glycine receptor subunit (GlyRα1), and calretinin, a marker of the AII amacrine cell in primate retina (Wässle et al., 1995; Kolb et al., 2002). Figure 9 shows examples of DB1 cells that showed clear contacts with putative AII amacrine cells. The arrowheads indicate locations where GlyRα1 puncta could be seen juxtaposed between a DB1 axon terminal and an AII amacrine cell lobular appendage in the OFF sublamina. These data suggest that DB1 cells, like FMB and DB3 cells (Grünert and Wässle, 1996; Jusuf et al., 2005), probably receive synaptic input from AII amacrine cells via GlyRα1.

DISCUSSION

In contrast to mouse, rat, and rabbit retina, where staining was found in numerous populations of cone bipolar cells (Puthussery et al., 2010), SCGN staining can be used as a marker of DB1 bipolar cells in the macaque retina. In addition, a heterogeneous population of GABAergic amacrine cells showed expression of this protein. An interaction of SCGN with SNAP-25 (25 kDa synaptosomeassociated protein) has been reported (Rogstam et al., 2007), suggesting a possible role in exocytosis; however, the precise functional role of SCGN is unknown, and therefore we will focus our discussion on the use of SCGN as a marker of the DB1 bipolar cell.

SCGN is a marker of DB1 in the macaque retina

Several lines of evidence indicate that the SCGN-positive OFF cone bipolar cells represent the DB1 bipolar cell described by Boycott and Wässle (1991). First, these cells had axon terminals that stratified in the most distal region of the IPL (stratum 1). Second, consistent with Boycott and Wässle's description of DB1 cells, the terminal arbor was relatively wide and comprised several fine branches with intermittent swellings along the process, arranged like "pearls on a string." In contrast, the FMB and DB2 cells have a narrower axonal arbor and larger, more bulbous axonal varicosities arranged like "grapes on a vine." On average, 6.4 cones contacted each SCGN-positive OFF cone bipolar cell in the mid-peripheral retina, consistent with a previous more limited analysis for the DB1 (5–8, Boycott and Wässle, 1991).

The strong staining of the DB1 dendrites permitted investigation of the cone connectivity and glutamate receptor expression of these cells. Such an analysis is precluded for other OFF cone bipolar cell markers in the macaque, such as calbindin (marker of DB3) and recoverin (marker of FMB), which label photoreceptors in addition to a specific population of bipolar cells. In the IPL, SCGN was localized to amacrine cell processes as well as to bipolar cell axon terminals. We found that it was possible to distinguish the DB1 axon terminals from the amacrine cell processes by double labeling with vGluT1, which stains bipolar axon terminals, or by careful reconstruction from confocal images.

In addition to DB1 bipolar cells, we observed SCGN staining in occasional ON cone bipolar cells. The intensity of staining was weak compared with the DB1 staining and double labeling with vGluT1 indicated that SCGN was absent from the axon terminals of these ON bipolar cells. Moreover, our nearest neighbor analysis showed a regularly arranged mosaic of bipolar cells, suggesting that we successfully avoided erroneously counting the weakly stained ON bipolar or amacrine cell somata. Thus, for light microscopy, the weak ON bipolar cell staining is unlikely to have confounded our analysis of DB1 contacts. At the ultrastructural level, we occasionally observed invaginating contacts between SCGN-positive bipolar cells and cone pedicles. Although Hopkins and Boycott (1996) reported sparse invaginating contacts for a DB1 cell (3 out of 74 contacts), it seems more likely that such contacts originated from SCGN-positive ON cone bipolar cells, and that they were more readily detected at the EM level due to the signal amplification used for preembedding immunohistochemistry.

Photoreceptor connectivity of DB1

We found that DB1 bipolar cells make indiscriminate contacts with all cone pedicles within reach, confirming previous reports for this bipolar cell type (Boycott and Wässle, 1991). This is in contrast to other primate bipolar cell types, such as the DB3 bipolar, which appear to be biased against S-cone contacts, in that they often avoid contacts with S-cones within the reach of their dendritic arbor (Lee and Grünert, 2007). Thus, the center response of the DB1 bipolar cell is expected to comprise a luminance signal without spectral bias. Interestingly, the putative homologs in mouse (Type 1, Ghosh et al., 2004) and ground squirrel (cb1 or former b7, Puller et al., 2011) appear to follow the more general pattern in that they avoid blue cones and selectively contact L/M-cones (Li and DeVries, 2006; Breuninger et al., 2011). Although we did observe rare examples of DB1 contacts with rod photoreceptors, such contacts were only seen at ≈0.03% of rod photoreceptors and were not made by all DB1 cells. Thus, it seems likely that such contacts represent an aberration rather than a typical feature of DB1 circuitry.

Glutamate receptors of DB1

In the primate OPL, the AMPA receptor subunit GluA1 is found exclusively at flat contacts made by OFF cone bipolar cell dendrites at the base of the cone pedicle, and is largely restricted to TA contacts (Haverkamp et al., 2000). In the marmoset retina, FMB cells express GluA1 at ≈56% of their dendritic tips (Puller et al., 2007). In contrast, in this study we could not identify a candidate glutamate receptor subunit that was present in the majority of DB1 dendritic tips. Staining for GluA3 and SGCN was not performed, since a recent study has demonstrated complete colocalization of this subunit with GluA4 (Puller and Haverkamp, 2011). The two other kainate receptor subunits that were not tested here, GluK4 and GluK5, have not yet been successfully localized in primate retina; however, neither of these subunits is thought to be capable of forming a functional ion channel in the absence of GluK1, 2 or 3 (Ren et al., 2003; Nasu-Nishimura et al., 2006). In summary, the subunit composition of the glutamate receptor expressed at the dendritic tips of DB1 bipolar cells remains unclear. It is possible that our methods were not sensitive enough to detect low-level expression of these proteins. The synaptic response in the putative homolog in ground squirrel retina, the b7 cell, is sensitive to SYM2081 and is therefore likely to be kainatemediated (DeVries, 2000). An alternative explanation is that the DB1 could signal through a glutamate transporter as has been shown previously for cone bipolar cells in teleost retina (Grant and Dowling, 1995). Indeed, we demonstrate here that the DB1 bipolar does express the glutamate transporter GLT-1 (see Fig. 3G–I); however, this did not seem to be concentrated to the dendritic tips near the site of glutamate release. Future studies, employing double-labeling immunoelectron microscopy and/or electrophysiological studies, will be required to determine the mechanism of light-evoked signaling in the DB1 bipolar cell.

Pre- and postsynaptic partners at DB1 axon terminals

Functional studies have established that the AII amacrine cell mediates crossover inhibition from the ON pathway to the OFF pathway, via glycinergic synapses onto the OFF bipolar cell terminals (Molnar et al., 2009). Under scotopic conditions, this connection carries the rod signal from the rod bipolar cells into the OFF cone bipolar cells, but it remains uncertain whether the AII amacrine cells make connections with all types of OFF cone bipolar cells. Our triple-labeling studies (Fig. 9) demonstrate the presence of the α1 glycine receptor subunit at points of contact between AII amacrine cell dendrites and DB1 bipolar cell axon terminals. Previous studies in macaque retina indicate that the FMB and DB3 type bipolar cells also express GlyRa1 at sites that make contact with AII amacrine cells (Grünert and Wässle, 1996; Jusuf et al., 2005). Thus, at present we can say that scotopic signals likely reach DB1, DB3, and FMB bipolar cells via the AII amacrine cells; the DB2 remains to be tested. It should be noted that although the calretinin antibody was shown to be a marker of the AII amacrine cell in macaque (Wässle et al., 1995), a subsequent study revealed that an additional population of glycinergic amacrine cells is also labeled (Kolb et al., 2002). Although we made efforts to avoid these cells in our analysis (see Materials and Methods), it remains possible that some GlyRa1 puncta observed on the DB1, at points of contact with CalR-immunoreactive amacrine cells, could represent synaptic inputs from a glycinergic amacrine cell type other than the AII amacrine cell.

What are the postsynaptic partners at the DB1 output synapse? Although the intrinsically photoreceptive M1-melanopsin ganglion cells as well as the dopaminergic amacrine cells stratify in the S1 region of the IPL, electrophysiological recordings indicate that these cells exhibit a physiological ON response to light stimulation (Dacey et al., 2005; Zhang et al., 2007). Furthermore, recent anatomical evidence suggests that both of these cell types receive *en passant* synapses from ON cone bipolar cell axons (Dumitrescu et al., 2009; Hoshi et al., 2009; Grünert et al., 2011). Thus, it seems unlikely that these cells receive

inputs from the DB1 bipolar. The dendritic arbors of the OFF parasol ganglion cell are narrowly stratified in S2, at ≈30% depth of the IPL (Jacoby and Marshak, 2000; Jacoby et al., 2000; Bordt et al., 2006), and are therefore highly unlikely to receive any input from DB1. Similarly, the small bistratified cells are predominantly stratified within S2 and are thought to derive bipolar cell inputs from DB2 and DB3 bipolar cells (Calkins et al., 1998; Ghosh and Grünert, 1999; Bordt et al., 2006). The OFF type large sparse monostratified ganglion cell stratifies in S1 of the IPL. The ON variant of this cell has been studied physiologically and shows S-OFF and LM-ON opponency; however, the physiology of the OFF type has not yet been described (Dacey et al., 2003). Thus, further studies will be necessary to establish the postsynaptic partners of this OFF cone bipolar cell type.

Supplementary Material

Refer to Web version on PubMed Central for supplementary material.

Acknowledgments

We thank G.-S. Nam for technical assistance and G. Adamus, R.F. Margolskee, J. Nathans, D. Pow, and L. Wagner for providing antibodies.

Grant sponsor: National Institutes of Health (NIH); Grant number: EY017095 (to W.R.T.); Grant sponsor: Deutsche Forschungsgemeinschaft (DFG); Grant number: HA 5277/2-2 (to S.H.); Grant sponsor: NHMRC (Australia); Grant number: Postdoctoral Fellowship 520033 (to T.P.); Grant sponsor: Research to Prevent Blindness to the Department of Ophthalmology, OHSU.

LITERATURE CITED

Adamus G, Amundson D. Epitope recognition of recoverin in cancer associated retinopathy: evidence for calcium-dependent conformational epitopes. J Neurosci Res. 1996; 45:863–872. [PubMed: 8892098]

Bloomfield SA, Dacheux RF. Rod vision: pathways and processing in the mammalian retina. Prog Retin Eye Res. 2001; 20:351–384. [PubMed: 11286897]

Bordt AS, Hoshi H, Yamada ES, Perryman-Stout WC, Marshak DW. Synaptic input to OFF parasol ganglion cells in macaque retina. J Comp Neurol. 2006; 498:46–57. [PubMed: 16856174]

Boycott BB, Hopkins JM. Cone synapses of a flat diffuse cone bipolar cell in the primate retina. J Neurocytol. 1993; 22:765–778. [PubMed: 8270960]

Boycott BB, Wässle H. Morphological classification of bipolar cells of the primate retina. Eur J Neurosci. 1991; 3:1069–1088. [PubMed: 12106238]

Brandstätter JH, Koulen P, Wässle H. Selective synaptic distribution of kainate receptor subunits in the two plexiform layers of the rat retina. J Neurosci. 1997; 17:9298–9307. [PubMed: 9364075]

Breuninger T, Puller C, Haverkamp S, Euler T. Chromatic bipolar cell pathways in the mouse retina. J Neurosci. 2011; 31:6504–6517. [PubMed: 21525291]

Calkins DJ, Tsukamoto Y, Sterling P. Microcircuitry and mosaic of a blue-yellow ganglion cell in the primate retina. J Neurosci. 1998; 18:3373–3385. [PubMed: 9547245]

Dacey DM, Packer OS. Colour coding in the primate retina: diverse cell types and cone-specific circuitry. Curr Opin Neurobiol. 2003; 13:421–427. [PubMed: 12965288]

Dacey DM, Liao HW, Peterson BB, Robinson FR, Smith VC, Pokorny J, Yau KW, Gamlin PD. Melanopsin-expressing ganglion cells in primate retina signal colour and irradiance and project to the LGN. Nature. 2005; 433:749–754. [PubMed: 15716953]

DeVries SH. Bipolar cells use kainate and AMPA receptors to filter visual information into separate channels. Neuron. 2000; 28:847–856. [PubMed: 11163271]

Dhingra A, Sulaiman P, Xu Y, Fina ME, Veh RW, Vardi N. Probing neurochemical structure and function of retinal ON bipolar cells with a transgenic mouse. J Comp Neurol. 2008; 510:484–496. [PubMed: 18671302]

Dowling JE, Boycott BB. Organization of the primate retina: electron microscopy. Proc R Soc Lond B Biol Sci. 1966; 166:80–111. [PubMed: 4382694]

Drenckhahn D, Holbach M, Ness W, Schmitz F, Anderson LV. Dystrophin and the dystrophin-associated glycoprotein, beta-dystroglycan, co-localize in photoreceptor synaptic complexes of the human retina. Neuroscience. 1996; 73:605–612. [PubMed: 8783274]

Dumitrescu ON, Pucci FG, Wong KY, Berson DM. Ectopic retinal ON bipolar cell synapses in the OFF inner plexiform layer: contacts with dopaminergic amacrine cells and melanopsin ganglion cells. J Comp Neurol. 2009; 517:226–244. [PubMed: 19731338]

Fyk-Kolodziej B, Qin P, Pourcho RG. Identification of a cone bipolar cell in cat retina which has input from both rod and cone photoreceptors. J Comp Neurol. 2003; 464:104–113. [PubMed: 12866131]

Ghosh KK, Grünert U. Synaptic input to small bistratified (blue-ON) ganglion cells in the retina of a new world monkey, the marmoset Callithrix jacchus. J Comp Neurol. 1999; 413:417–428. [PubMed: 10502249]

Ghosh KK, Bujan S, Haverkamp S, Feigenspan A, Wässle H. Types of bipolar cells in the mouse retina. J Comp Neurol. 2004; 469:70–82. [PubMed: 14689473]

Gong J, Jellali A, Mutterer J, Sahel JA, Rendon A, Picaud S. Distribution of vesicular glutamate transporters in rat and human retina. Brain Res. 2006; 1082:73–85. [PubMed: 16516863]

Grant GB, Dowling JE. A glutamate-activated chloride current in cone-driven ON bipolar cells of the white perch retina. J Neurosci. 1995; 15:3852–3862. [PubMed: 7538566]

Grünert U, Wässle H. GABA-like immunoreactivity in the macaque monkey retina: a light and electron microscopic study. J Comp Neurol. 1990; 297:509–524. [PubMed: 2384611]

Grünert U, Wässle H. Glycine receptors in the rod pathway of the macaque monkey retina. Vis Neurosci. 1996; 13:101–115. [PubMed: 8730993]

Grünert U, Martin PR, Wässle H. Immunocytochemical analysis of bipolar cells in the macaque monkey retina. J Comp Neurol. 1994; 348:607–627. [PubMed: 7530731]

Grünert U, Jusuf PR, Lee SC, Nguyen DT. Bipolar input to melanopsin containing ganglion cells in primate retina. Vis Neurosci. 2011; 28:39–50. [PubMed: 20950505]

Hack I, Peichl L, Brandstätter JH. An alternative pathway for rod signals in the rodent retina: rod photoreceptors, cone bipolar cells, and the localization of glutamate receptors. Proc Natl Acad Sci U S A. 1999; 96:14130–14135. [PubMed: 10570210]

Haverkamp S, Grünert U, Wässle H. The cone pedicle, a complex synapse in the retina. Neuron. 2000; 27:85–95. [PubMed: 10939333]

Haverkamp S, Grünert U, Wässle H. The synaptic architecture of AMPA receptors at the cone pedicle of the primate retina. J Neurosci. 2001a; 21:2488–2500. [PubMed: 11264323]

Haverkamp S, Grünert U, Wässle H. Localization of kainate receptors at the cone pedicles of the primate retina. J Comp Neurol. 2001b; 436:471–486. [PubMed: 11447590]

Haverkamp S, Specht D, Majumdar S, Zaidi NF, Brandstätter JH, Wasco W, Wässle H, Tom Dieck S. Type 4 OFF cone bipolar cells of the mouse retina express calsenilin and contact cones as well as rods. J Comp Neurol. 2008; 507:1087–1101. [PubMed: 18095322]

Hokoc JN, Mariani AP. Tyrosine hydroxylase immunoreactivity in the rhesus monkey retina reveals synapses from bipolar cells to dopaminergic amacrine cells. J Neurosci. 1987; 7:2785–2793. [PubMed: 2887643]

Hoshi H, Liu WL, Massey SC, Mills SL. ON inputs to the OFF layer: bipolar cells that break the stratification rules of the retina. J Neurosci. 2009; 29:8875–8883. [PubMed: 19605625]

Huang L, Shanker YG, Dubauskaite J, Zheng JZ, Yan W, Rosenzweig S, Spielman AI, Max M, Margolskee RF. Ggamma13 colocalizes with gustducin in taste receptor cells and mediates IP3 responses to bitter denatonium. Nat Neurosci. 1999; 2:1055–1062. [PubMed: 10570481]

Huang L, Max M, Margolskee RF, Su H, Masland RH, Euler T. G protein subunit G gamma 13 is coexpressed with G alpha o, G beta 3, and G beta 4 in retinal ON bipolar cells. J Comp Neurol. 2003; 455:1–10. [PubMed: 12454992]

Jacoby RA, Marshak DW. Synaptic connections of DB3 diffuse bipolar cell axons in macaque retina. J Comp Neurol. 2000; 416:19–29. [PubMed: 10578100]

Jacoby RA, Wiechmann AF, Amara SG, Leighton BH, Marshak DW. Diffuse bipolar cells provide input to OFF parasol ganglion cells in the macaque retina. J Comp Neurol. 2000; 416:6–18. [PubMed: 10578099]

Johnson J, Tian N, Caywood MS, Reimer RJ, Edwards RH, Copenhagen DR. Vesicular neurotransmitter transporter expression in developing postnatal rodent retina: GABA and glycine precede glutamate. J Neurosci. 2003; 23:518–529. [PubMed: 12533612]

Jusuf PR, Haverkamp S, Grünert U. Localization of glycine receptor alpha subunits on bipolar and amacrine cells in primate retina. J Comp Neurol. 2005; 488:113–128. [PubMed: 15924342]

Kalloniatis M, Marc RE, Murry RF. Amino acid signatures in the primate retina. J Neurosci. 1996; 16:6807–6829. [PubMed: 8824321]

Kolb H. Organization of the outer plexiform layer of the primate retina: electron microscopy of Golgi-impregnated cells. Philos Trans R Soc Lond B. 1970; 258:261–283. [PubMed: 22408829]

Kolb H, Zhang L, Dekorver L, Cuenca N. A new look at calretinin-immunoreactive amacrine cell types in the monkey retina. J Comp Neurol. 2002; 453:168–184. [PubMed: 12373782]

Lee SC, Grünert U. Connections of diffuse bipolar cells in primate retina are biased against S-cones. J Comp Neurol. 2007; 502:126–140. [PubMed: 17335043]

Li W, DeVries SH. Bipolar cell pathways for color and luminance vision in a dichromatic mammalian retina. Nat Neurosci. 2006; 9:669–675. [PubMed: 16617341]

Li W, Keung JW, Massey SC. Direct synaptic connections between rods and OFF cone bipolar cells in the rabbit retina. J Comp Neurol. 2004; 474:1–12. [PubMed: 15156575]

Li W, Chen S, DeVries SH. A fast rod photoreceptor signaling pathway in the mammalian retina. Nat Neurosci. 2010; 13:414–416. [PubMed: 20190742]

Mariani AP, Hokoc JN. Two types of tyrosine hydroxylase-immunoreactive amacrine cell in the rhesus monkey retina. J Comp Neurol. 1988; 276:81–91. [PubMed: 2903868]

Martin PR, Grünert U. Analysis of the short wavelength-sensitive (“blue”) cone mosaic in the primate retina: comparison of New World and Old World monkeys. J Comp Neurol. 1999; 406:1–14. [PubMed: 10100889]

Mataruga A, Kremmer E, Muller F. Type 3a and type 3b OFF cone bipolar cells provide for the alternative rod pathway in the mouse retina. J Comp Neurol. 2007; 502:1123–1137. [PubMed: 17447251]

Milam AH, Dacey DM, Dizhoor AM. Recoverin immunoreactivity in mammalian cone bipolar cells. Vis Neurosci. 1993; 10:1–12. [PubMed: 8424920]

Molnar A, Hsueh HA, Roska B, Werblin FS. Crossover inhibition in the retina: circuitry that compensates for nonlinear rectifying synaptic transmission. J Comput Neurosci. 2009; 27:569–590. [PubMed: 19636690]

Nasu-Nishimura Y, Hurtado D, Braud S, Tang TT, Isaac JT, Roche KW. Identification of an endoplasmic reticulum-retention motif in an intracellular loop of the kainate receptor subunit KA2. J Neurosci. 2006; 26:7014–7021. [PubMed: 16807331]

Park SA, Yin H, Bhattarai JP, Park SJ, Lee JC, Kim CJ, Han SK. Postnatal change of GluR5 kainate receptor expression in the substantia gelatinosa neuron of the trigeminal subnucleus caudalis in mice. Brain Res. 2010; 1346:52–61. [PubMed: 20513362]

Pfeiffer F, Simler R, Grenningloh G, Betz H. Monoclonal antibodies and peptide mapping reveal structural similarities between the subunits of the glycine receptor of rat spinal cord. Proc Natl Acad Sci U S A. 1984; 81:7224–7227. [PubMed: 6095276]

Pow DV, Hendrickson AE. Distribution of the glycine transporter glyt-1 in mammalian and nonmammalian retinae. Vis Neurosci. 1999; 16:231–239. [PubMed: 10367958]

Puller C, Haverkamp S. Cell-type-specific localization of protocadherin beta16 at AMPA and AMPA/Kainate receptor-containing synapses in the primate retina. J Comp Neurol. 2011; 519:467–479. [PubMed: 21192079]

Puller C, Haverkamp S, Grünert U. OFF midget bipolar cells in the retina of the marmoset, Callithrix jacchus, express AMPA receptors. J Comp Neurol. 2007; 502:442–454. [PubMed: 17366611]

Puller C, Ondreka K, Haverkamp S. Bipolar cells of the ground squirrel retina. J Comp Neurol. 2011; 519:759–774. [PubMed: 21246553]

Puthussery T, Gayet-Primo J, Taylor WR. Localization of the calcium-binding protein secretagogin in cone bipolar cells of the mammalian retina. J Comp Neurol. 2010; 518:513–525. [PubMed: 20020539]

Ren Z, Riley NJ, Garcia EP, Sanders JM, Swanson GT, Marshall J. Multiple trafficking signals regulate kainate receptor KA2 subunit surface expression. J Neurosci. 2003; 23:6608–6616. [PubMed: 12878702]

Rogstam A, Linse S, Lindqvist A, James P, Wagner L, Berggard T. Binding of calcium ions and SNAP-25 to the hexa EF-hand protein secretagogin. Biochem J. 2007; 401:353–363. [PubMed: 16939418]

Schroder S, Hoch W, Becker CM, Grenningloh G, Betz H. Mapping of antigenic epitopes on the alpha 1 subunit of the inhibitory glycine receptor. Biochemistry. 1991; 30:42–47. [PubMed: 1703015]

Tsukamoto Y, Morigiwa K, Ueda M, Sterling P. Microcircuits for night vision in mouse retina. J Neurosci. 2001; 21:8616–8623. [PubMed: 11606649]

Vardi N. Alpha subunit of Go localizes in the dendritic tips of ON bipolar cells. J Comp Neurol. 1998; 395:43–52. [PubMed: 9590545]

Wagner L, Oliyarnyk O, Gartner W, Nowotny P, Groeger M, Kaserer K, Waldhausl W, Pasternack MS. Cloning and expression of secretagogin, a novel neuroendocrineand pancreatic islet of Langerhans-specific Ca2+-binding protein. J Biol Chem. 2000; 275:24740–24751. [PubMed: 10811645]

Wang Y, Macke JP, Merbs SL, Zack DJ, Klaunberg B, Bennett J, Gearhart J, Nathans J. A locus control region adjacent to the human red and green visual pigment genes. Neuron. 1992; 9:429–440. [PubMed: 1524826]

Wässle H, Chun MH. Dopaminergic and indoleamineaccumulating amacrine cells express GABA-like immunoreactivity in the cat retina. J Neurosci. 1988; 8:3383–3394. [PubMed: 2902202]

Wässle H, Riemann HJ. The mosaic of nerve cells in the mammalian retina. Proc R Soc Lond B Biol Sci. 1978; 200:441–461. [PubMed: 26058]

Wässle H, Grünert U, Martin PR, Boycott BB. Immunocytochemical characterization and spatial distribution of midget bipolar cells in the macaque monkey retina. Vision Res. 1994; 34:561–579. [PubMed: 8160377]

Wässle H, Grünert U, Chun MH, Boycott BB. The rod pathway of the macaque monkey retina: identification of AII-amacrine cells with antibodies against calretinin. J Comp Neurol. 1995; 361:537–551. [PubMed: 8550898]

Winsky L, Isaacs KR, Jacobowitz DM. Calretinin mRNA and immunoreactivity in the medullary reticular formation of the rat: colocalization with glutamate receptors. Brain Res. 1996; 741:123–133. [PubMed: 9001714]

Zhang DQ, Zhou TR, McMahon DG. Functional heterogeneity of retinal dopaminergic neurons underlying their multiple roles in vision. J Neurosci. 2007; 27:692–699. [PubMed: 17234601]

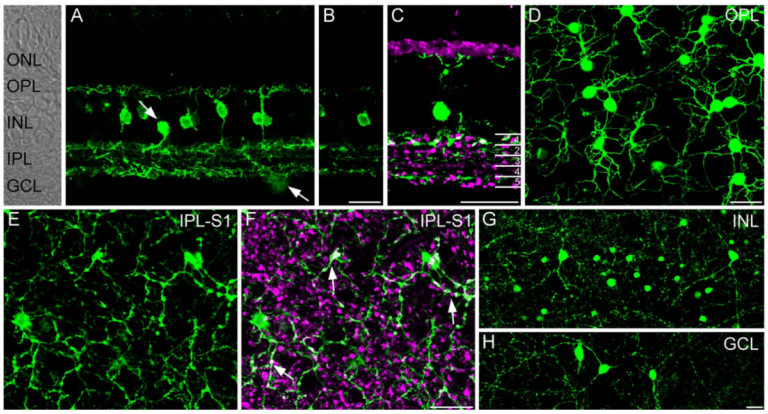

Figure 1.

Localization of SCGN in the peripheral macaque retina. A: Confocal projection (7 ×0.8 μm) of a vertical section of macaque retina stained for SCGN. Labeling is present in the soma, dendrites, and axons of a population of bipolar cells and in occasional putative amacrine cells in the inner nuclear layer and ganglion cell layer (arrows). Retinal layers are indicated on the transmitted light image to the left side of panel A. **B**: Single confocal plane of the same area shown in **A**. Note that SCGN-positive processes are concentrated in three major bands at the top, middle, and bottom of the IPL. **C**: Confocal projection (4 ×0.9 μm) of vertical section stained with vGluT1 and SCGN shows that some SCGN-positive processes in S1 were also immunoreactive for vGluT1, while processes outside of S1 lacked vGluT1 immunoreactivity. Numbers on the right-hand side of panel delineate the five IPL strata. **D**: Confocal projection of wholemount retina (5 × 0.4 μm) stained for SCGN and focused at the level of the OPL. Strong SCGN immunoreactivity is present in diffuse bipolar cell dendrites. **E**: Confocal projection (3 ×0.4 μm) of wholemount retina stained for SCGN and focused at the level of S1 of the IPL. **F**: Same region as in E showing staining for SCGN and vGluT1. SCGN-positive bipolar cell terminals show vGluT1 immunoreactivity (white, arrows). These terminals are fine, with intermittent swellings arranged like “pearls on a string.” Other vGluT1-positive bipolar cell terminals are more bulbous in appearance. Note that many SCGN-stained processes in this focal plane are not vGluT1-positive, and are likely of amacrine cell origin. **G,H**: Confocal projections (5 ×0.9 μm), showing wide-field amacrine cells with somata located in the inner nuclear layer (G) and ganglion cell layer (H). Amacrine cells showed diverse morphology and, in some cases, had dendrites spanning over 0.5 mm. Scale bars = 20 μm. [Color figure can be viewed in the online issue, which is available at wileyonlinelibrary.com.]

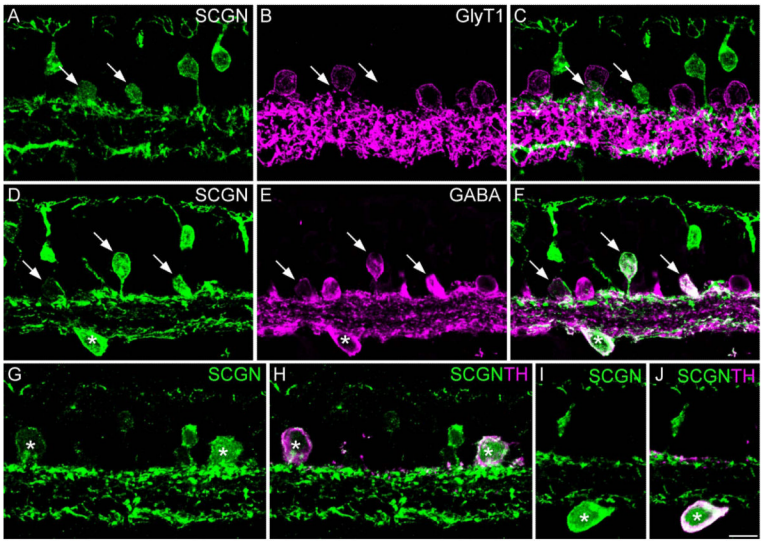

Figure 2.

SCGN is localized to multiple GABAergic amacrine cell types. Confocal images of vertical sections from peripheral retina stained for SCGN and various amacrine cell markers. **A–C**: Confocal projection (6 ×0.9 μm) showing staining with SCGN (A) and GlyT1 (B). The merged panel (C) shows that SCGN-positive amacrine cells (arrows) lack glycine transporter immunoreactivity. **D–F**: Confocal projection (5 × 0.9 μm) showing that SCGN-positive amacrine cells in the INL (arrows) are also immunoreactive for GABA. SCGN-positive somata in the GCL are also GABA-immunoreactive (asterisk). **G–J**: Confocal projections (2 × 0.9 μm) showing examples of SCGN-positive amacrine cells in the INL (G,H) and GCL (I,J) that also show immunoreactivity for tyrosine hydroxylase (TH). Scale bar = 10 μm. [Color figure can be viewed in the online issue, which is available at wileyonlinelibrary.com.]

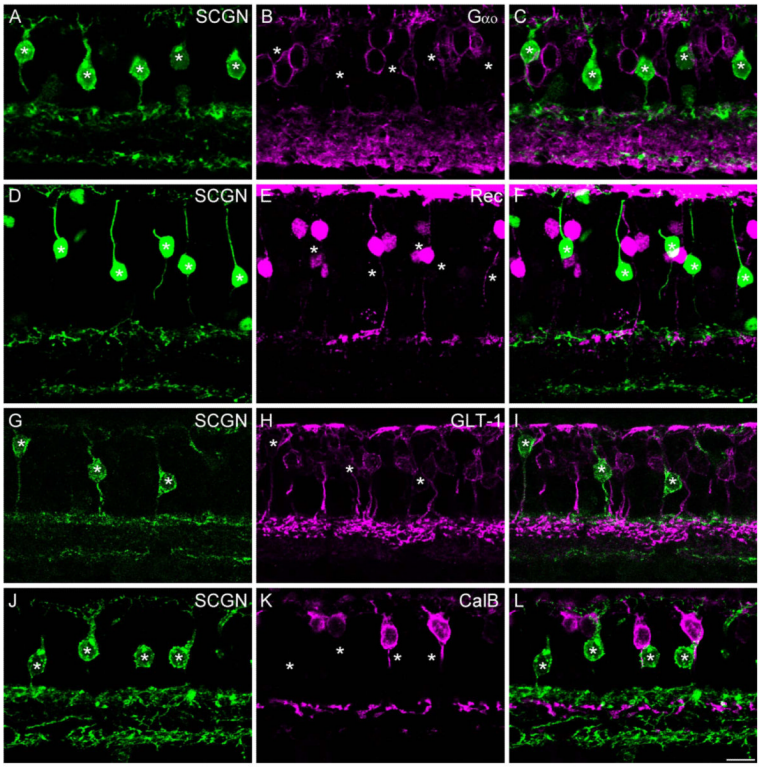

Figure 3.

SCGN is localized to DB1 bipolar cells. Confocal projections of vertical sections labeled for SCGN (left panels) and various OFF bipolar cell markers (middle panels). Merged images are shown in the right-hand panels. **A–C**: Intensely labeled SCGN-positive bipolar cells (asterisks) lack $G\alpha_o$ staining, indicating that they are likely OFF cone bipolar cells (projection of 7 × 0.4 μm). **D–F**: SCGN-positive bipolar cells (asterisks) do not colocalize with the flat midget bipolar cell marker, recoverin (projection of 7 × 0.9 μm). **G–I**: Staining for SCGN and GLT-1, a marker of DB2 and FMB bipolar cells. SCGN-positive bipolar cells (asterisks) show weak GLT-1 immunoreactivity; however, the more intensely stained DB2 axon terminals are in a more proximal position in the IPL (projection of 3 × 1.0 μm). **J–L**: Staining for SCGN and the DB3 marker, calbindin. SCGN-positive bipolar cells (asterisks) lack calbindin immunoreactivity (6 ×0.9 μm). All images are from peripheral retina except **D–F**, which is taken from mid-peripheral retina. Scale bar = 10 μm. [Color figure can ≈be viewed in the online issue, which is available at wileyonlinelibrary.com.]

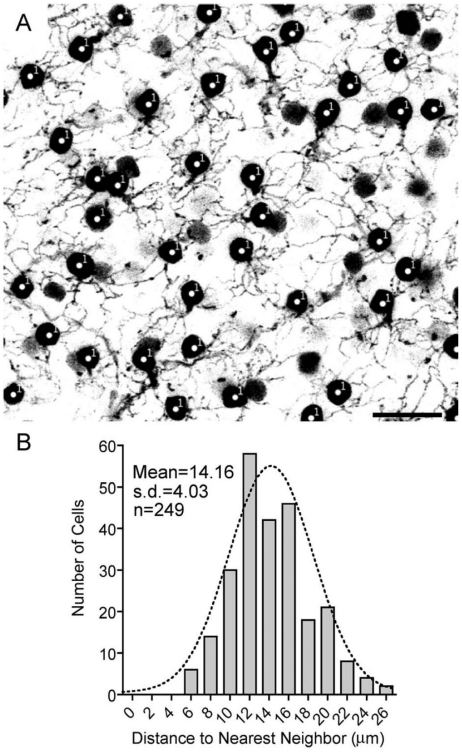

Figure 4.

DB1 bipolar cells form a regular mosaic. **A**: Confocal projection (10 ×1.25 μm) showing a representative field from mid-peripheral retina used for nearest-neighbor analysis. The focal plane extends from the distal INL to the OPL. Bipolar cell somata (indicated with #1) and dendrites are visible. Other more weakly stained somata lacked dendrites and were likely amacrine cells. B: Frequency histogram showing distance to nearest neighbor for DB1 somata. The dotted line indicates a Gaussian distribution with a mean of 14.16 μm, which provides a good fit to the data, and indicates a regularly arranged mosaic of cell bodies. Scale bar = 20 μm.

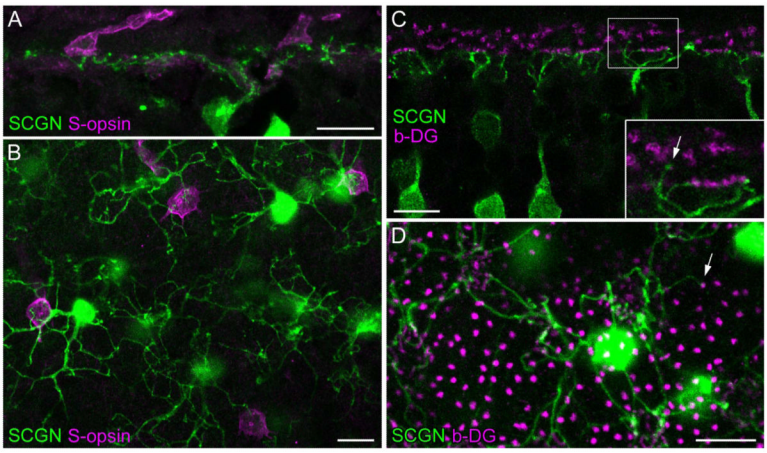

Figure 5.

DB1 bipolar cells frequently contact S-cones but rarely contact rods. **A**: Confocal projection (3 × 1.0 μm) of a peripheral retinal section stained for SCGN and S-opsin showing that SCGN-labeled bipolar cell dendrites contact two S-cone pedicles. **B**: A single confocal section showing double labeling of SCGN and S-opsin in whole-mounted mid-peripheral retina. SCGN-labeled DB1 bipolar cells nonselectively contact M/L cones and S-cone pedicles within their dendritic arbors. **C,D**: Double labeling of SCGN and β-dystroglycan (b-DG, as a marker for rod terminals and cone pedicles) on a vertical section (C, single confocal image) and whole-mount (projection of 2 × 1.0 μm) from mid-peripheral retina. Rare examples of SCGN-positive dendrites that appeared to contact rod terminals are indicated (arrows). Scale bars = 10 μm. [Color figure can be viewed in the online issue, which is available at wileyonlinelibrary.com.]

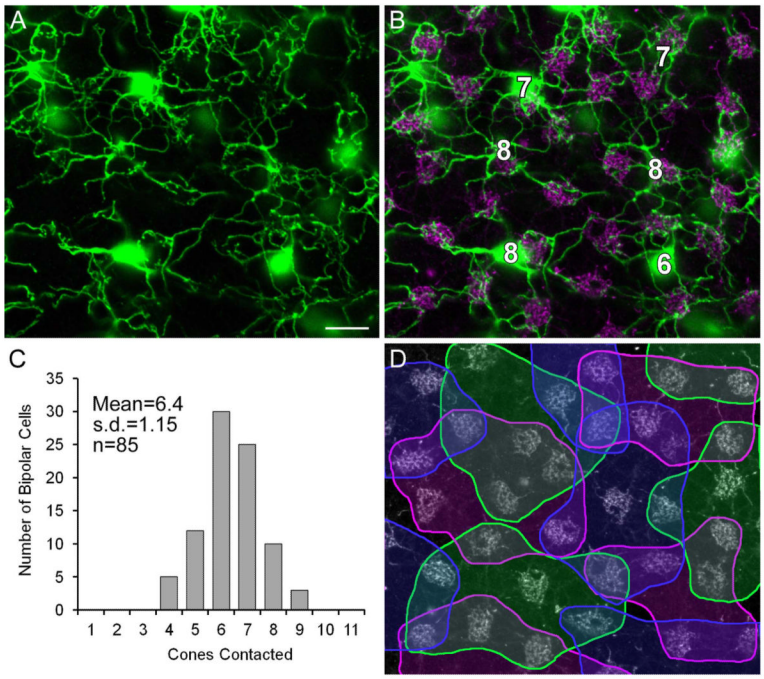

Figure 6.

Cone contacts of DB1 bipolar cells. **A**: Projection of horizontal sections of retina (3 × 0.6 μm) showing dendritic trees of neighboring DB1 cells in mid-peripheral retina. **B**: Same field as in A, cone pedicles are labeled with GluK1. DB1 cells were in contact with 6–8 cones. **C**: Frequency histogram of the number of cone contacts of individual DB1 cells. **D**: Same field as in A with colored outlines defining the cone pedicles contacted by each DB1 cell. Note that several cone pedicles are contacted by 2–3 DB1 cells and one cone pedicle is contacted by four DB1 cells. Scale bar = 10 μm. [Color figure can be viewed in the online issue, which is available at wileyonlinelibrary.com.]

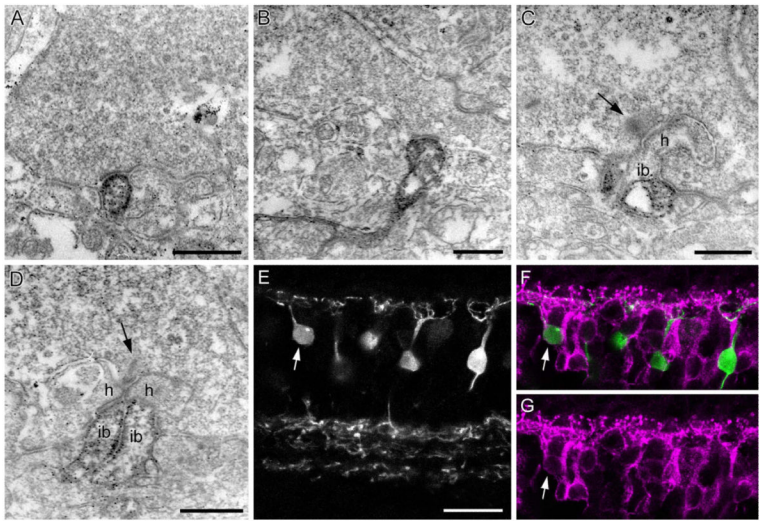

Figure 7.

Synaptic contacts of DB1 cells at the cone pedicle. Flat contacts at the base of the cone pedicle are subdivided into triad-associated (TA) or nontriad-associated (NTA) contacts, depending on the relative distance from the triad. **A,B**: Preembedding electron micrographs of cone pedicles with SCGN-labeled dendrites making NTA contacts. **C**: SCGN immunoreactivity is localized to the TA position on both sides of the triad. No immunoreactivity is seen at the invaginating ON bipolar cell (ib) or horizontal cell dendrites (h). The presynaptic ribbon is indicated by arrow. *D*: Example of weak immunoreactivity in two invaginating dendrites of putative ON bipolar cells (ib). **E–G**: Confocal projection (2 ×1.0 μm) of a section stained for SCGN, shown in E, and Gγ13, shown in G, merge in F. Most SCGN-positive bipolar cells are Gγ13-negative; arrow marks one Gγ13-positive bipolar cell. Scale bars = 0.5 μm in A–D; 20 μm in E. [Color figure can be viewed in the online issue, which is available at wileyonlinelibrary.com.]

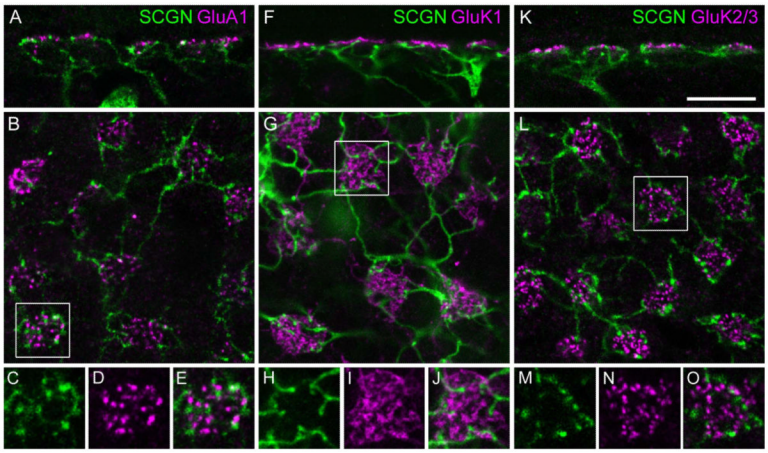

Figure 8.

Glutamate receptors of DB1 bipolar cells. Localization of AMPA and kainate receptor subunits at cone pedicles in confocal images of vertical (A,F,K) and horizontal sections (B,G,L) from mid-peripheral retina. **A–E**: Most dendritic tips of DB1 bipolar cells, which are labeled with SCGN, do not colocalize with GluA1-immunoreactive puncta. **F–J**: GluK1 immunoreactivity is localized between the dendritic tips of DB1. **K–O**: GluK2/3 puncta do not overlap with SCGN labeling. All images are confocal projections (A, 2 × 1.0 μm; B, 4 × 0.6 μm; F, 2 ×0.6 μm; G, 3 ×0.6 μm; K, 2 ×0.6 μm; L, 4 ×0.3 μm). Scale bar = 10 μm in K (for A,B,F,G,K,L). [Color figure can be viewed in the online issue, which is available at wileyonlinelibrary.com.]

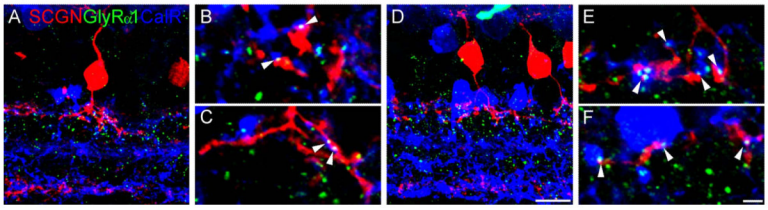

Figure 9.

DB1 bipolar cells express glycine receptors at points of contact with putative AII amacrine cells. **A,D**: Confocal projections of vertical sections from peripheral retina (7 ×0.44 μm) stained for SCGN, the glycine receptor GlyRα1, and the AII amacrine cell marker, calretinin. Note the diffuse morphology of the DB1 axon terminals. **B,C**: Single confocal image planes from the cell shown in A. **E,F**: Single confocal image planes from the cell shown in D. Arrowheads indicate regions where GlyRα1 puncta are positioned at points of cofasciculation between DB1 axon terminals and putative AII amacrine cell lobular appendages. Scale bars 10 = μm (large panels); 2 μm (subpanels). [Color figure can be viewed in the online issue, which is available at wileyonlinelibrary.com.]

TABLE 1

Primary Antibodies

Antibody	Immunogen	Source, catalog no.	Species	Dilution
β-dystroglycan	C-terminus of human β-dystroglycan (PKNMTPYRSPP-PYVP) (Drenckhahn et al., 1996)	Novocastra, Newcastle upon Tyne, UK #NCL-b-DG 8 (Clone 43DAG1/8D5)	Mouse, monoclonal	1:100
Calbindin-D-28K	Purified bovine kidney calbindin-D-28K	Sigma, St. Louis, MO #C9848	Mouse, monoclonal	1:3,000
Calretinin	Rat calretinin	Millipore, Billerica, MA #AB1550	Goat, polyclonal	1:1,000
GABA	GABA coupled to KLH via glutaraldehyde	Millipore, Billerica, MA #AB175	Guinea Pig, polyclonal	1:5,000
GluA1 (GluR1)	C-terminus of rat GluR1 (SHSSGMPLGATGL)	Chemicon, Temecula, CA #AB1504	Rabbit, polyclonal	1:100
GluA2 (GluR2)	Synthetic peptide corresponding to C-terminal amino acids (840-886) of human GluR2	FabGennix International Inc., Frisco, TX #GluR2-201AP	Rabbit polyclonal	1:100
GluA4 (GluR4)	Synthetic peptide corresponding to the C-terminus of rat glutamate receptor 4 (GluR4) subunit (RQSSGLA-VIASDLP) conjugated to bovine serum albumin (BSA) with glutaraldehyde	Millipore, Billerica, MA#AB1508	Rabbit polyclonal	1:500
GluK1 (GluR5)	C-terminus of human GluR5 (KLIREERGIRKQSSVHTV)	Santa Cruz, Heidelberg, Germany #SC-7616	Goat, polyclonal	1:100
GluK2/3 (GluR6/3)	C-terminus of rat GluR6 (KHTFNDRRLPGKETMA)	Upstate, Lake Placid, NY #06-309	Rabbit, polyclonal	1:1,000
GLT-1 (EAAT2)	C-terminal amino acids 554-573 of rat precursor gluta-mate transporter GLT-1	Tocris, Ellisville, MO #2063	Rabbit, polyclonal	1:1,000
Glycine receptor alpha 1 subunit (GlyRa1)	Purified rat spinal cord glycine receptor	Synaptic Systems, Göttingen, Germany #146 111 (Clone mAb2b)	Mouse, monoclonal	1:100
Glycine transporter 1 (GlyT1)	Synthetic peptide corresponding to the final 15 amino acids at the carboxyl terminus of GlyT-1 conjugated to to thryoglobulin with formaldehyde (Pow and Hendrickson, 1999)	Gift from Dr. D. Pow, University of Queensland, Bris-bane, Australia	Rabbit, polyclonal	1:4,000
$G\alpha_o$	Partially purified bovine brain $G\alpha_o$ protein	Biomol International, Enzo Life Sciences, PA #SA280 Clone mAB2A.3	Mouse, monoclonal	1:1,000
Gγ13	G protein Gγ13, peptide sequence CFLNPDLMKNNPWV	Gift from Dr. R. F. Margolskee, Mount Sinai School of Medicine, New York, NY	Rabbit, polyclonal	1:1,000
Recoverin (Rec-1)	Purified recoverin (Adamus and Amundson, 1996)	Gift from Dr. G. Adamus, Casey Eye Institute, Portland, OR	Rat, monoclonal	1:200
S-cone opsin	Last 42 AA of the human blue pigment (JH455, Wang et al., 1992)	Gift from Dr. J. Nathans, John Hopkins University, Balti-more, MD	Rabbit, polyclonal	1:5000
Secretagogin	Full length (276AA) recombinant Human Secretagogin + 10 AA N-term Histidine-tag	Biovendor R&D, Candler, NC (#RD181120100)	Rabbit, polyclonal	1:5,000
Secretagogin	Recombinant human secretagogin (Wagner et al., 2000)	Gift from Dr. L. Wagner, University of Vienna, Austria	Rabbit, polyclonal	1:5,000
Secretagogin	Full length (276AA) recombinant Human Secretagogin + 10AA N-term Histidine-tag	Biovendor R&D, Candler, NC (#RD184120100)	Sheep, polyclonal	1:2,000

Antibody	Immunogen	Source, catalog no.	Species	Dilution
Tyrosine hydroxylase	Purified tyrosine hydroxylase from PC12 cells	Millipore, Billerica, MA #MAB318	Mouse, monoclonal	1:1,000
vGluT1	Synthetic peptide (aa 542-560 of rat vGlut1)	Millipore, Billerica, MA #AB5905	Guinea pig, polyclonal	1:5,000

TABLE 2

List of Abbreviations Used in Figures

b-DG, beta dystroglycan
CalB, calbindin
CalR, calretinin
GABA, gamma aminobutyric acid
Gao, G protein o, alpha subunit
GCL, ganglion cell layer
GLT-1, glutamate transporter 1
GluA1, AMPA type glutamate receptor 1 subunit (formerly known as GluR1)
GluK1, kainate type glutamate receptor 5 subunit (formerly known as GluR5)
GluK2/3, kainate type glutamate receptor 2/3 subunit (formerly known as GluR6/7)
GlyRa1, glycine receptor alpha 1 subunit
GlyT1, glycine transporter 1
INL, inner nuclear layer
IPL, inner plexiform layer
ONL, outer nuclear layer
OPL, outer plexiform layer
Rec, recoverin
S1, stratum 1
SCGN, secretagogin
TH, tyrosine hydroxylase